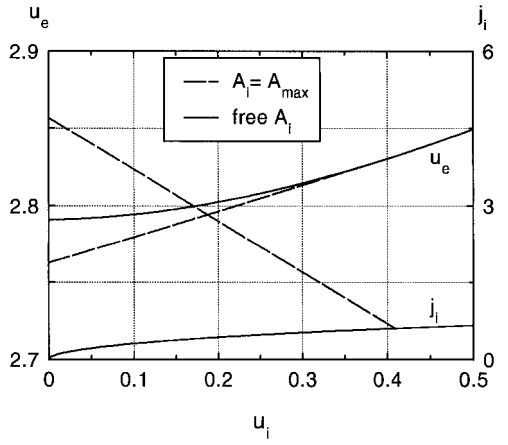

Fig. 3 Influence of the inlet velocity ($A_{max} = 10$).

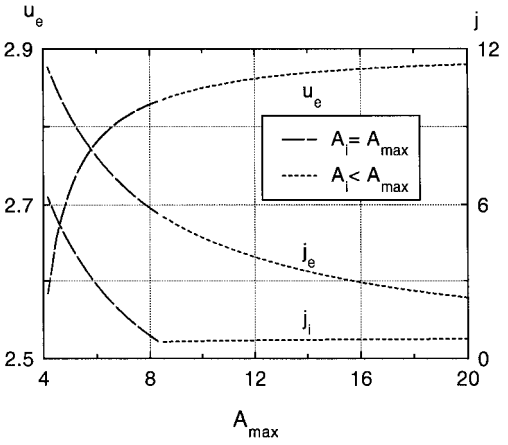

Fig. 4 Influence of the area limit ($u_i = 0.5$).

and Eq. (7) concordantly provide $j_e = 1.355$, whereas a small benefit on the exit velocity ($u_e = 2.8835$) is obtained. The inaccuracy of Toki's results is confirmed by searching for the optimal geometry of a thruster that presents a constant-area appendage with the same $A_{max} = 34.70$, as in Toki's geometry. The numerical solution provides $u_e = 2.8858$ and, obviously, $j_e = 1.355$.

The constraint $A_e = A_{max}$ is in fact always necessary; to be consistent, one should at least impose an equal limit on the initial cross section. The same value $A_{max} = 10$ is considered in Fig. 3, which points out the influence of the inlet velocity; the channel begins with a constant-area duct if $u_i < 0.4$. The initial peak of the current density is more plausibly removed by specifying a high u_i than by exploiting the optimization process. Unfortunately, the increase of the initial velocity does not produce the same increase in the exit velocity, and the engine thrust decreases; the engine efficiency, which depends on the square of the plasma velocity, is instead improved.

The same initial velocity $u_i = 0.5$ is considered in Fig. 4; a larger value of A_{max} produces better performance and reduces both the current-density peaks. The left extremes of the curves in Fig. 4 ($A_{max} = 4.17$) correspond to a constant-area channel that becomes convergent-divergent as soon as A_{max} is increased. The improvement of the thruster characteristics gradually diminishes, and $A_{max} = 10$ seems to be a suitable compromise between engine performance and dimensions.

Conclusions

The theory of optimal control has been applied to the analysis of a MPD thruster by using a simple quasi-one-dimensional model that neglects the energy equation. A correct solution of the unconstrained problem has been presented and discussed. The introduction of a constraint concerning the maximum value of the channel cross-section area has provided more realistic results; nevertheless, a more precise model that takes the energy equation into account would be opportune. The optimization of the plasma final velocity does not imply the smoother distribution of the current density that has been asserted in recent literature. The practical goal of OCT application is only the fast design of the channel geometry that ensures high specific impulse for specified values of the discharge voltage and total current. In the authors' opinion the improvement of theoretical knowledge is, however, the main outcome of an indirect optimization procedure.

References

[1]Toki, K., "Optimal Control of Quasi-One-Dimensional Self-Field Magnetoplasmadynamic Arcjet Flowfields," *Journal of Propulsion and Power*, Vol. 13, No. 1, 1997, pp. 157–161.

[2]Kuriki, K., Kunii, Y., and Shimizu, Y., "Idealized Model for Plasma Acceleration in an MHD Channel," *AIAA Journal*, Vol. 21, No. 3, 1983, pp. 322–326.

[3]Cicala, P., *An Engineering Approach to the Calculus of Variations*, 2nd ed., Levrotto and Bella, Turin, Italy, 1997, pp. 10–12.

[4]Bryson, A. E., and Ho, Y.-C., *Applied Optimal Control* (rev. printing), Hemisphere, Washington, DC, 1975, pp. 47–49.

Transonic Compressor Influences on Upstream Surface Pressures with Axial Spacing

Peter J. Koch,* Douglas P. Probasco,* and J. Mitch Wolff†
Wright State University, Dayton, Ohio 45435
William W. Copenhaver‡
Air Force Research Laboratory,
Wright Patterson Air Force Base, Ohio 45433
and
Randall M. Chriss§
NASA Lewis Research Center, Cleveland, Ohio 44135

Introduction

GAS turbines are a vital energy source for both industrial and military applications, with recent research focusing on identifying high cycle fatigue unsteady flow mechanisms. There is a constant need for improved understanding of the flow physics through the various components. Greater understanding of these mechanisms provides manufacturers with the ability to achieve higher levels of performance and more efficient systems. As the level of technology increases, there are continuous demands on gas turbine engines to achieve greater durability, reduced noise levels, size, and, of course, greater thrust. A considerable portion of recent research involves the unsteady interaction between adjacent blade rows in both compressor and turbine sections.

The objective of this research is to investigate and quantify the fundamental vane/blade interaction phenomena of the upstream traveling potential forcing function from a downstream rotor in a compression system. This is accomplished by performing a series of

Received 12 April 1999; revision received 13 April 2000; accepted for publication 12 December 2000.

*Graduate Research Assistant, Department of Mechanical and Material Engineering. Student Member AIAA.

†Assistant Professor, Department of Mechanical and Material Engineering. Senior Member AIAA.

‡Principal Research Engineer, Air Force Research Laboratory, Propulsion Directorate, Turbine Engine Division. Fellow AIAA.

§Aerospace Engineer, Research and Technology Directorate, Turbomachinery and Propulsion Systems Division. Associate Fellow AIAA.

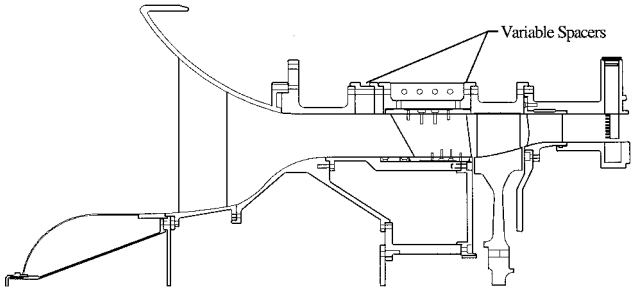

Fig. 1 Schematic of flow path.

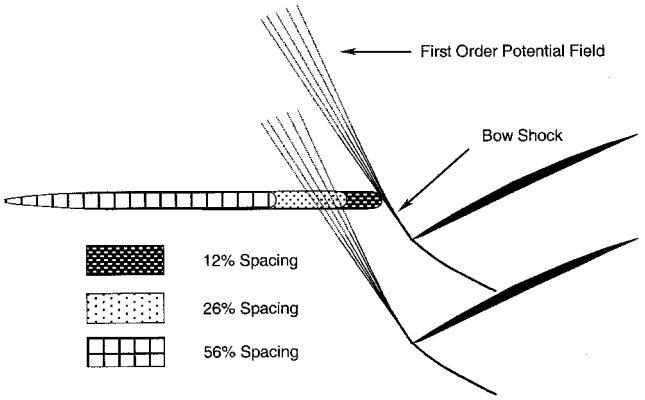

Fig. 2 IGV/rotor interaction.

experiments in the Compressor Aero Research Laboratory (CARL), a high-speed, highly loaded compression stage facility. During testing inlet guide vane (IGV) unsteady surface pressure measurements were taken at different IGV/rotor spacings while operating at 105% design speed.

Research Compressor

The research compressor (Fig. 1) was designed to simulate the second stage of a highly loaded military core compressor. Wakes from a first stage are simulated with an upstream blade row. The primary intent for the use of the research compressor was to investigate the influence of an upstream stage on the flow swallowing capability of a downstream transonic stage. The rotor has 33 blades and operates at a design tip relative Mach number of 1.19. Further details of the compressor design can be found in Ref. 1.

To study the effect of different upstream stages, an IGV assembly is placed upstream of the rotor section. These IGVs were designed to create a wake consistent with a modern technology, highly loaded, low-aspect-ratio stage and to maintain an axial inlet flow orientation. Therefore, they have a wide bluff trailing edge as shown in Fig. 2. They have a constant solidity (spacing-to-chord ratio) along the span and have no steady aerodynamic loading to achieve a uniform two-dimensional wake. In addition, it is possible to vary the axial spacing between the IGVs and the rotor. The three different spacings possible are 12, 26, and 56% of the IGV chord measuring from the IGV trailing edge to the rotor leading edge. In the current configuration there are 24 IGVs in the upstream passage.

IGV Surface Pressure Instrumentation

To measure the unsteady surface pressures the IGVs are instrumented with miniature Kulite pressure transducers. Two different blades are instrumented with 10 pressure transducers each. Spanwise effects were also investigated by instrumenting the blade at two different spanwise locations, 50 and 75% from the hub. The pressure transducers are flush mounted by machining the blade surface, and the diaphragm is then covered with a thin layer of room temperature vulcanizing silicone rubber to protect the sensor. Grooves were also machined into the surface so that the lead wires could be bundled and fed out through the case without disturbing the flow. Two adjacent IGVs are instrumented providing data for one flow passage. Flow periodicity is assumed with one blade's data phase shifted to the other blade for analysis.

LQ-125 miniature pressure transducers from Kulite are used to measure the surface pressure. The pressure transducers are manufactured directly on the blades with a 172.4-kPa maximum absolute pressure capability. The pressure sensing element is 0.1524 cm in diameter and has an internally compensated temperature range from -1.1 to 54.4°C. The natural frequency of the pressure transducer is 300 kHz, giving a usable frequency range of 75 kHz. The measured random uncertainty was ± 0.69 kPa, which includes all errors due to random noise and temperature changes.

Results

A series of experiments were performed to investigate the IGV unsteady surface pressure response due to the upstream traveling pressure field generated by the downstream rotor. The variable spacing feature of the experimental rig was used to study the effect that changing the axial spacing has on the unsteady IGV surface pressure measured at two spanwise locations.

The experimental data were recorded on a 28-channel analog tape recorder with a flat response up to 80 kHz. The data was digitized offline at an effective sample rate of 500 kHz by reducing the tape playback speed by one-quarter and sampling at 125 kHz. The first 11 blade pass harmonics are resolved without aliasing or attenuation. Data were digitized for a time record of 68 ms as was dictated by storage limitations, which gives approximately 11 rotor revolutions. Ensemble averaging was performed on the data to average out any inconsistencies that may exist from one rotor blade to the next. The ensemble averaging was accomplished by using the rotor blade pass frequency and, because the rotor has 33 blades, about 363 records were ensemble averaged. To assist in discussing the results, two blade passages of data are presented from the single averaged passage record.

To analyze the effect that axial spacing has on the upstream IGV surface pressures, a 105% design speed, peak efficiency operating point was used. This operating point produces rotor relative Mach numbers of 1.22 and 1.15 for the 75 and 50% spans, respectively. A nondimensionalized difference of the pressure values across the blade was determined from the measured absolute pressure data as defined by Eq. (1):

$$p_n = (p_1 - p_2)/p_s \tag{1}$$

where the subscripts are defined as follows: n, normalized pressure; s, IGV inlet; 1, IGV upper surface; and 2, IGV lower surface.

Axial Spacing Influences

Figure 3 shows the 50% span, 95% chord location results. The 12% IGV chord axial spacing shows an unsteady normalized force of 0.39 (31.8 kPa), which is larger than the 0.20 (15.9 kPa) loading found at the 26% axial spacing. However, the 56% IGV chord axial spacing data show a substantially smaller normalized force of 0.09 (7.25 kPa) on the blade when compared to the closer spacings.

As shown in Fig. 3, there is a significant change in the unsteady loading with changes in axial spacing. These types of phenomena are important to engine designers because typically no upstream unsteady loading is considered during the structural analysis of an engine. Therefore, with the continued push for smaller and lighter engines, where axial spacings have decreased from approximately 50 to 25% of blade chord, these unsteady loads experienced by the upstream row must now be considered during engine design.

Figure 3 also shows the phase shift, relative to the rotor leading edge, with changes in axial spacing. Figure 3 clearly shows that the 12% IGV chord spacing leads the other axial spacings in phase. This is because at the 12% spacing the rotor bow shock contacts the IGV surface earlier because of the decreased distance it has to travel before reaching the IGV trailing edge.

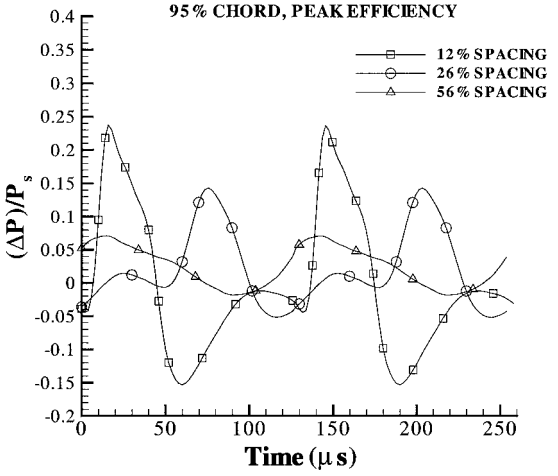

Fig. 3 Differenced nondimensionalized pressure time traces for three axial spacings: 50% span, 95% chord.

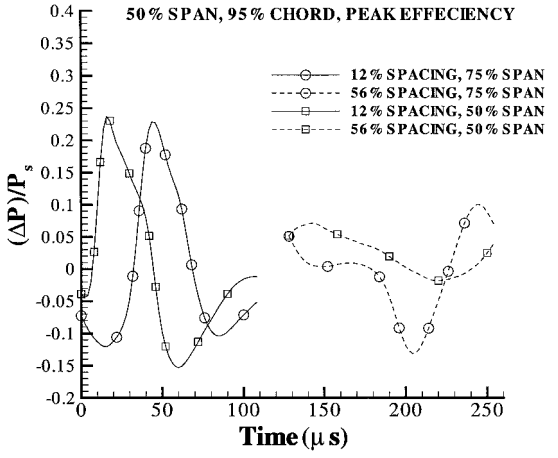

Fig. 4 Differenced nondimensionalized pressure time traces for 95% chord.

Figure 2 shows how, relative to a rotor blade position, the bow shock impinges on the 12% spaced IGV prior to the 26 and 56% spacings. Figure 2 also demonstrates how the shock dissipates in the upstream direction from a sharp discontinuity in pressure producing high-order harmonic loads on the close spacing IGV, to a weak pressure wave with primarily first-order loading as the IGV spacing is increased.

The 50% span results reveal several trends. First, axial spacing variations have a significant effect on the upstream traveling unsteady pressure fluctuations generated by the downstream transonic rotor. Therefore, unsteady loading on the upstream blade row should be included in the design of gas turbines, especially as the axial spacing decreases. Second, an overall decrease in the unsteady loading occurs as we move upstream along the IGV surface for each spacing. Finally, there is a change in phase with changes in axial spacing.

Spanwise Variations

To determine whether any radial variations affect the flow physics of the upstream traveling interaction, data at 50 and 75% span are utilized. Figure 4 shows the 50 and 75% span location results for time traces of the unsteady delta pressure at 12 and 56% spacing for a common chordwise location. Figure 4 shows that the 75% span unsteady loading is 0.35 (28.4 kPa) at 12% spacing, which is slightly smaller than the loading at 50% span. However, the pressure fluctuation at 56% spacing for 75% span is significantly greater than the loading at 50% span, from 0.23 (18.9 kPa) to 0.09 (7.25 kPa), respectively.

All of the trends found at 50% span were also evident in the 75% span results. However, spanwise variations in the compressor stage

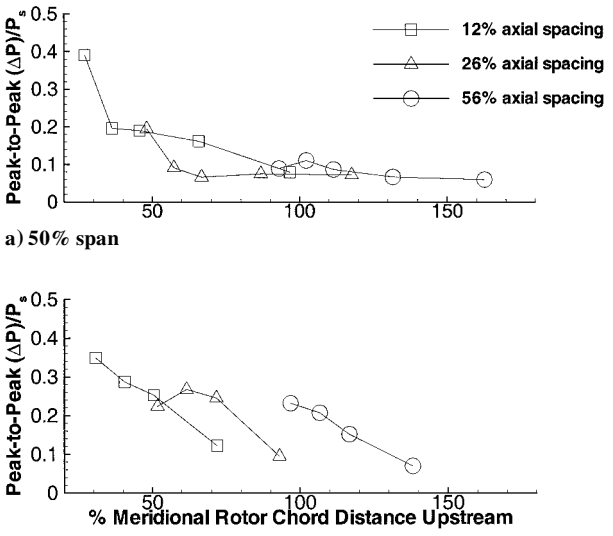

Fig. 5 Chordwise variation in peak pressure loading.

are evident as shown by comparison of the results shown in Fig. 4. In general, the unsteady pressure loading is greater at 75% span than at 50% span, whereas dissipation of the unsteady loading with axial spacing was less at 75% span than at 50%. Therefore, the upstream propagating unsteady pressure fluctuation persists farther upstream at the larger span location. This could be attributed to the higher relative Mach number at the 75% span.

Chordwise Variations

Figure 5 shows the influence of absolute upstream position on the measured blade surface peak-to-peak unsteady pressure for both spanwise locations and each IGV axial spacing. Figure 5a, at 50% span suggests that the peak-to-peak pressure loading tends to collapse regardless of IGV axial spacing for locations greater than 100% rotor chord distances upstream of the rotor. However, at 75% span (Fig. 5b) no evidence of this phenomena can been seen upstream through distances of 150% of the rotor chord. Because the peak-to-peak pressure loading does not collapse to one value at a given absolute axial location, the IGV cannot be considered a passive device in the flowfield, with no influence on the rotor upstream potential forces. Instead Fig. 5 shows that for both 50 and 75% span the IGVs interact with the rotor potential field and their axial spacing influences the measured peak-to-peak pressure forces. This experiment demonstrates the importance, in this case, of modeling the IGV/rotor interaction accurately, rather than assuming a simple exponential decay of the rotor potential field.

Conclusions

A series of experiments were performed to investigate the unsteady upstream traveling forcing function from a high-speed, highly loaded compressor rotor. These experiments were performed for several different axial spacings between the IGV and rotor rows, as well as at different spanwise locations. The IGV unsteady surface pressures were then measured to determine the forced response on the blade.

This investigation reveals several significant fundamental flow physics phenomena: 1) upstream traveling unsteady pressure fluctuations are significant, 2) the rotor bow shock dominates the pressure variations, and 3) changes in axial spacing affects the magnitude and character of the unsteady pressure loading.

References

[1] Law, C. H., "Two Axial Compressor Designs for a Stage Matching Investigation," Air Force Research Lab., AFWAL-TR-89-2005, Wright-Patterson AFB, OH, 1989.